Military Technical College
Kobry El-Kobbah,
Cairo, Egypt

14th International Conference on
Applied Mechanics and
Mechanical Engineering.

Aging response of Al-Zn-Mg 7020 alloy

By

M. Sabra** , M. Maher* , K. Almazy* and M. Sallam*

Abstract:

The aging response of Al-Zn-Mg alloy type 7020 was systemically studied including natural aging, one-stage aging, and two stages aging. The naturally aged alloy resulted in peak hardness of 113 HB, while one-step aging of the alloy at 120 °C for 28 hr, at 150 °C for 5 hrs, or at 200 °c for 20 min resulted in peak hardness of 109, 93, and 79 HB respectively. The two-stages aging was carried out at 120 °C as a low aging temperature and 150 °C as a high aging temperature and through different aging periods of time. When aging at 150 °C was preceded by a low temperature aging stage at 120 °C for different periods of time, the obtained hardness was increased and attained a peak value of 108 HB after 6 hrs at 120 °C and 8 hrs at 150°C. The analysis of the tensile fracture surface demonstrated dominating ductile dimple fracture modes in the solution treated specimens, while in the peak aged specimens some zones of cleavage brittle fracture were manifested together with the ductile fracture zones.

Keywords: aging, age hardening

* Egyptian Armed Forces
** Armed Forces Research Centre, ARC

1. Introduction:

The Al–Zn–Mg system offers the greatest potential of all aluminum alloys for age-hardening although the very high-strength alloys always contain quaternary additions of copper to improve their resistance to stress-corrosion cracking [1]. There is, however, an important range of medium strength alloys containing little or no copper that have the advantage of being readily weldable [2, 3] like 7020 type. These alloys differ from the other weldable aluminum alloys in that they age-harden significantly at room temperature [1, 4, 5]. Moreover, the strength properties that are developed are relatively insensitive to rate of cooling from high temperatures, and they possess a wide temperature range for solution treatment, i.e. 350 °C and above. Yield strengths may be as much as double those obtained for welded components made from the more commonly used Al–Mg and Al–Mg–Si alloys [1].

Al–Zn–Mg alloys were first developed for lightweight military bridges but they now have commercial applications like fast ships [1, 2]. Elsewhere, their use has been less widespread for fear of possible stress-corrosion cracking in the region of welds. The complete aging sequence in a wide range of ternary compositions [4, 6] is:

$$\alpha SSSS \rightarrow GP\ (Zn, Mg)\ zones \rightarrow \eta'\ (hexagonal) \rightarrow \eta\ (MgZn_2,\ hexagonal) \qquad (1)$$

The supersaturated sold solution (αSSSS) is obtained by a solution treatment followed by quenching to room temperature. The decomposition starts with the formation and growth of GP zones during the pre-aging treatment [6]. Two types of GP zones have been proposed to be formed in Al-Zn-Mg based alloys: solute rich GP I zones [7], for alloys with low Mg content; and solute/vacancy-rich GP II zones [7, 8, 9]. GPI zones are coherent with Al matrix with internal ordering of Zn and Al\Mg on the $\{100\}_{Al}$ planes, and are formed over a wide temperature range, from room temperature to 140-150 °C, independently of quenching temperature [10, 11]. GPII are zinc-rich layers on $\{111\}_{Al}$ planes and are formed after quenching from 450 °C and aging at temperature above 70 °C [4, 10]. Generally either GPI or both GPI and GPII zones can form as precursors to the metastable ή phase [11]. ή is semicoherent and η is incoherent [10, 11].

The purpose of the present article is to investigate the aging behavior and response of an aluminum alloy type 7020 and to understand the aging strengthening mechanism in different aging conditions. In the two-stages aging, the relative low aging temperature 120 °C was selected in this study to allow shorter and more practical aging time suitable for industrial purposes considering that the peak hardness obtained at this temperature differ only by less than 10 % of that obtained in natural aging after 60 days.

2. Experimental

The aluminum alloy 7020 was received in the form of rolled sheets with 10 mm thickness. The chemical composition (wt.%) of this alloy as analyzed by spectrometry is given in table (1) .

Table 1. Chemical composition of alloy 7020

	Zn%	Mg%	Ti%	Mn%	Fe%	Si%	Cu%	Al%
7020	4.7	1.2	0.036	0.3	0.25	0.23	0.065	rest

For the evaluation of the tensile characteristics of this aluminum alloy, standard flat tensile test specimens were cut by a wire-cut CNC machine. The specimens were machined according to ASTM specification E8. While for hardness evaluation 50X50 mm specimens with 10 mm depth were cut by the same machine and polished according to ASTM specification E10. The specimens were then solution treated at 450 °C for 2.5 hrs, water quenched to room temperature then the samples were heat treated naturally, or subjected to one-stag aging or two-stages aging. The naturally aged specimens were aged for 60 days. For the one-stag aging, the alloy was treated at 120, 150, 180, and 200 °C for several times up to 60 hrs. The two-stages aging consisted of an initial aging at 120 °C for different times up to 10 hrs, followed by a second aging cycle at 150 °C for various times up to 10 hrs.

The hardness test was done using Brinell hardness machine type . For the evaluation of the tensile characteristics a 100 KN Instron electro-hydraulic universal testing machine, model 8032, a Bluehill 2 software was used, to control the test and record the stress-strain curve and allows the determination of ultimate tensile strength and ductility. The fracture analysis was carried out using SEM type REMMA 202.

3. Results and Discussion

3.1 Natural aging treatment

Fig.(1) illustrates the natural aging response of the alloy 7020. At zero aging time which corresponds to the solid solution treated state the hardness was 54 HB. The hardness increases gradually with time to attain a max value of 115 HB after about 70 days (1200 hrs). It can be noted that a high rate of hardness increase is obtained in the initial stages of aging at room temperatures up to five days where the rate is substantially decreased to attain 113 HB after 50 days. This can be explained by the particular composition of the 7xxx Al-alloys series where Mg addition greatly reduces the low temperatures solubility of Zn in the Al-matrix which enhances and accelerates the formation of the spherical GP-zones usually formed in the early stages of aging. A. El Sheikh [12] indicated that these zones in this nucleation are mainly Zn clusters while Mg is introduced. The hardness gain when the aging time in prolonged to 70 days can be neglected then natural aging beyond 50 days is not worthy in these zones by diffusion through the vacancy mechanism, to allow an average Zn:Mg ratio of 4:1.

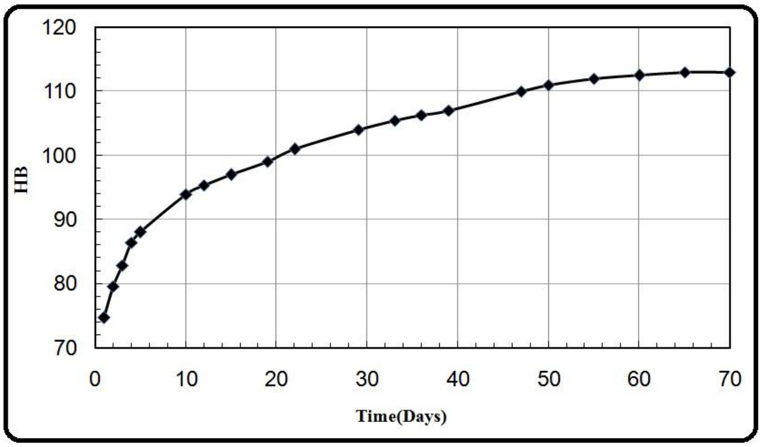

Fig. 1. The Aging Curve for Naturally Aged Specimen

3.2 One-step aging treatment

The aging curves for one-step aging are shown in Figs.(2),(3), and (4). The figures illustrate the aging response of the alloy at 120 °C, 150 °C, 180 °C, and 200 °C. The resulted hardness peak values were 109, 95, 83, and 79 HB, obtained after aging times of 28 hrs, 5hrs, 42 min. and 20 min respectively. It can be concluded that as the aging temperatures increases the aging time to reach the peak hardness decreases, moreover the value of at this peak hardness decreases. On the other hand, it can be noted that aging above 150 °C results in relatively low peak hardness values which can be manifested at very low aging times less than 45 min. Figs. (5), (6) summarize the effect of aging temperatures on the values of the obtained peak hardness and the aging times after which these peak values can be obtained.

To evaluate the mechanical tensile properties of the specimens subjected to a single aging cycle at different temperatures, a tensile tests were carried out on specimens peak aged at 120 °C and 150 °C together with a specimen solid solution treated only without aging as a term of comparison. Fig. (7) illustrates the obtained tensile curves of these specimens, where we can observe a clear serrated behavior on the flow curve of the solution treated specimens. In fact this behaviour is due to the dislocation-solute interaction (the repeated pinning and unpinning of moving dislocations by mobile solute atoms [13]). Due to the physical nature of this interaction, the extent of it is highly dependent on temperature and strain rate through the

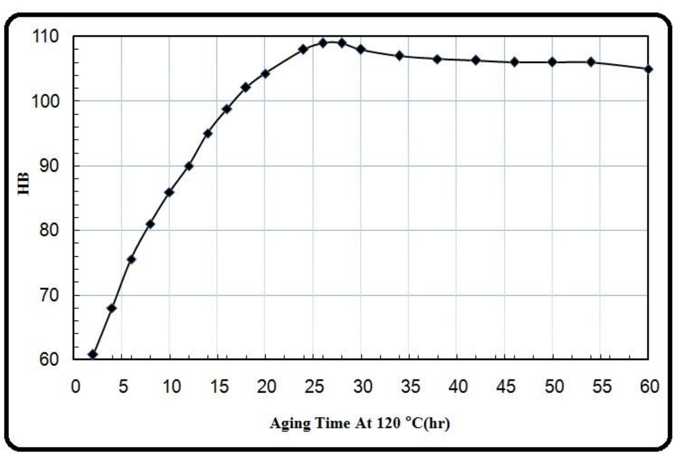

Fig. 2 Hardness as a function of aging time during one-stage aging at 120 °C

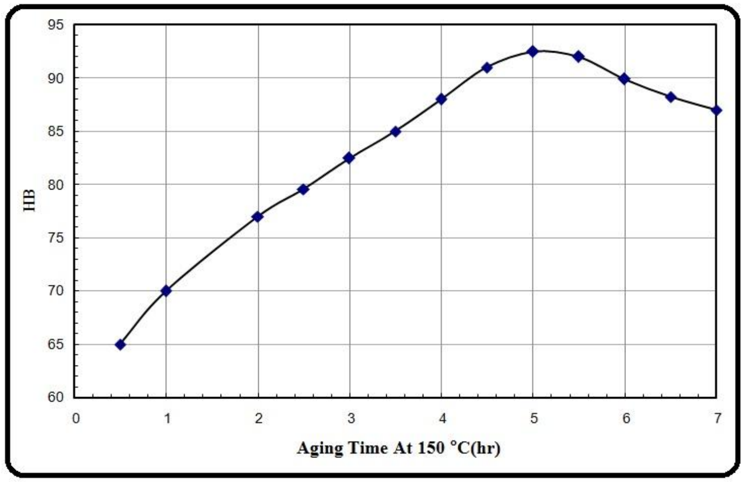

Fig. 3 Hardness as a function of aging time during one-stage aging at 150 °C

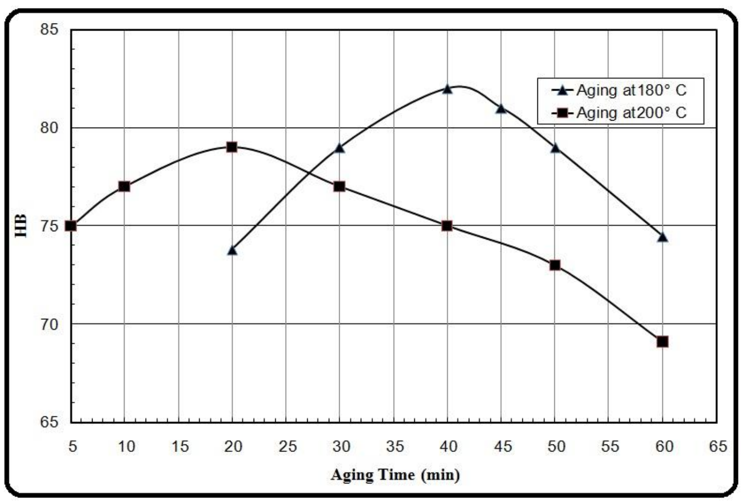

Fig. 4 Hardness as a function of aging time during one-stage aging at 180 °C and 200 °C

mechanisms of diffusion and thermal activation [13, 14]. This serration flow is called also the Portevin-Le Châtelier (PLC) effect, or serrated flow. Aluminum alloys are characterized by one type or two types of serrated flow characteristics (Portevin-Le Chatelier). The first called locking serration [7, 15], as an abrupt rise in flow stress followed by fall back to or below the level of the curve. This serration appears periodically and with an interval, ΔE1between two successive serrations. [7, 15] This kind of locking serration can also be identified in two forms, the first is A-type serration which is characterized by large interval between two successive serrations, and it is frequently observed in tensile tests of an aluminum alloy and related to the initial distribution of plastic hardness (or internal stress) along the specimen and to the way that this distribution is altered by deformation. When the distribution contains a hardness peak at a particular section of the specimen, because of a “natural” heterogeneity, a traveling Luders band may be forced to stop at that section and another band is then nucleated ahead of the heterogeneity leading to alternating serrations. The heterogeneity can be produced artificially by notching the specimen. It was found that there is a range of notch severity which results in alternating periodic serrations, with the bands stopping at the notch. For larger severities the tensile curve shows irregular non-periodic (type B) serrations, which is similar in form as the A-type serration but appears only in the internal between two A-type serration. The frequency of B-type serration is higher than that of A-type serration but its amplitude is relatively smaller. Locking serration mechanism type-A appears only at high strain rate > 1.66 x 10-4 sec-1 or at room temperature [7]. The second type of serration is called unlocking serration or C-type serration [7]. C-type serration is characterized by, at least initially, no increase in flow stress prior to discontinuous drop below the flow curve. This type of serration appears at high temperature and low strain rate. On this diagram we can observe the manifestation of serrated behavior in the case of solution treated state and we can recognize that it is a locking type A serration mechanisms where an abrupt rise in flow stress followed by a discontinues fall back to the level of the curve, while in specimens aged at 120 °C and 150 °C, we cannot reveal any visible serrated behavior. The ultimate tensile strength is increased by75% and 60% relative of the solution treated state in the specimens peak aged at 120 °C and 150 °C respectively. On the other hand the obtained ductily was notably reduced by about 32% and 20% also relative to the solution treated state in the specimens peak aged at 120 °C and 150 °C respectively.

3.3 Tow-step aging treatment

The tow-step aging comprise pre-aging for 2, 4, 6, 8, and 10 hrs at 120°c, followed by final aging at 150°c. The variation of hardness values after the final aging is plotted in Fig.(8). The tow-stags aging can provide the advantages of both low and high aging temperatures. Where the low temperature allow the formation of a large number of nucleation sites, while high aging temperature increase the rate of growth to reduce the aging time. Due to the relatively low values of the coefficient of diffusion at the low temperature of the first aging cycle, the aging time was prolonged from 2 hrs to 10 hrs. At the prescribed temperature of the second aging cycle the time was also varied from 1hr to 10 hrs to investigate the kinetics and the coherency of precipitates. In fact the low aging temperature cycle secure a nucleation regime allowing fine dispersed second phase particles, while the aging portion at relatively higher temperature enhances the growth process of these precipitates. Fig.(8 a) illustrates the effect of aging time during the final aging cycle at 150°c after an initial pre-aging aging cycle at 120 °C for 2, 4, and 6 hrs respectively on hardness values. As shown in the figure the peak values of the curves depend greatly on the aging time of low temperature aging cycle. We can note a significant difference of the obtained peak hardness values when the pre-aging times are varies from 2 to 6 hrs, while as shown in Fig.(8 b) the peaks are very near to each other. This means that until 4 hrs aging at 120°c there is more sites for nucleation is not occupied.

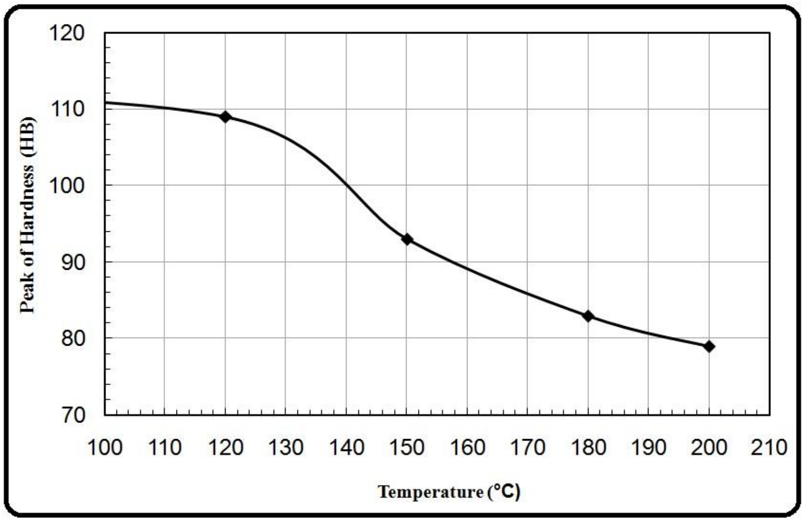

Fig. 5 Time to peak age hardness.

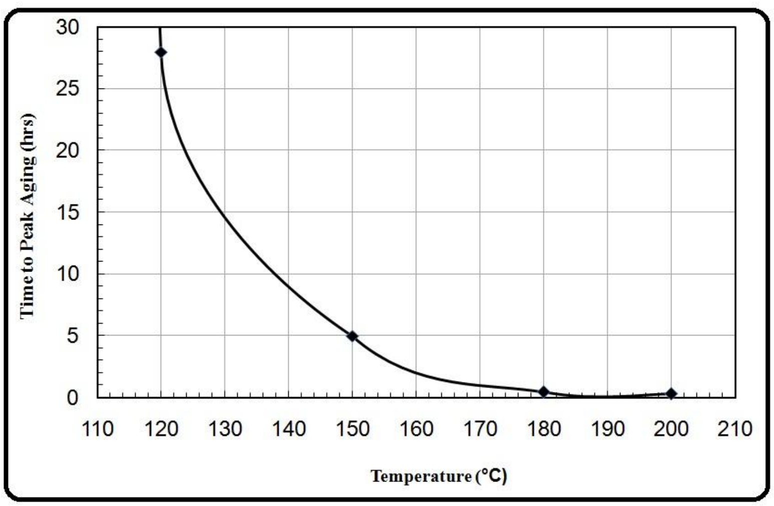

Fig. 6 Time to peak age hardness

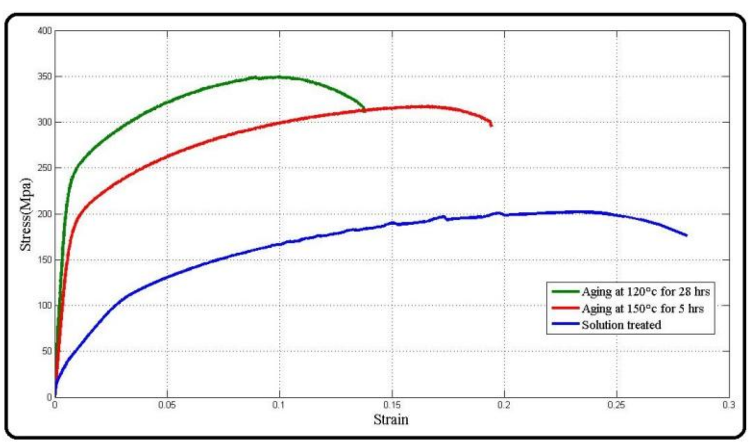

Fig. 7 Stress-strain curves of solution treated, aged at 120°c for 28 hrs, and aged at 150°c for 5 hrs

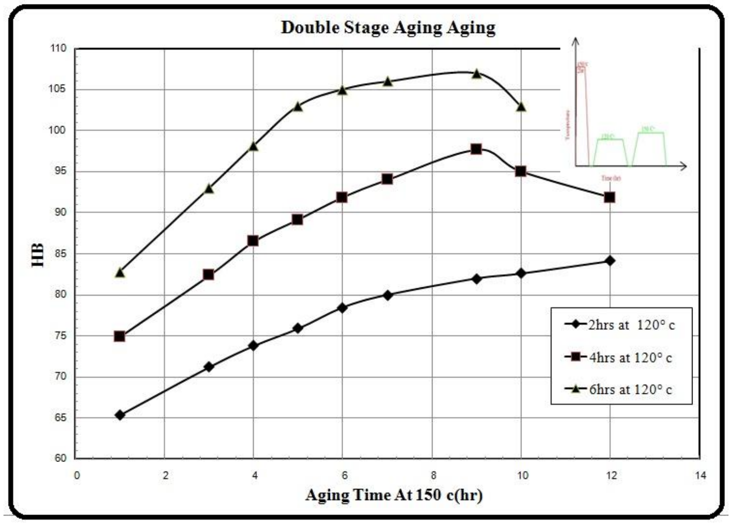

(a)

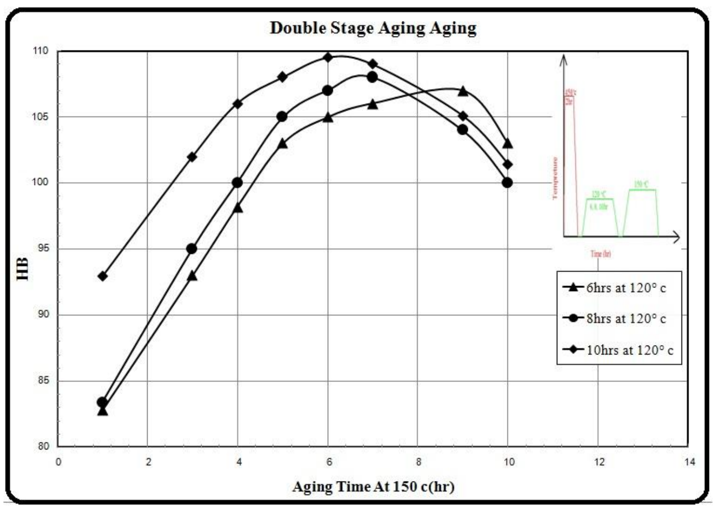

(b)

Fig. 8. Hardness as a function of aging time during tow-step aging at 150 °C

This means that nucleation and growth to GP zones takes about 6 hrs and the further aging time at this low aging temperature spend in growth of this nuclei to form η' then η. This result agrees with references [11, 16]

3.4 Fracture analysis

Figs.(9) (a) & (b) illustrate the tensile fracture obtained on specimens of the Aluminum alloy 7020 solution treated at 450 °C for 2.5 hrs. we can note that some large precipitates from previous aging heat treatment are still persisting and visible on the fracture. These precipitates have relatively coarse morphology and limited number, which indicates that theory were subjected to a high temperature cycle in fact, from the industrial point of view the adopted solid solution time (2.5 hrs) was chosen in order to dissolve most of the precipitates, but in the same time to keep the grain size within the fire grains limit, that is why solid solution holding time was not prolonged beyond 2.5 hrs. the prevailing mode of fracture is in its majority of dimple type, which indicates that the fracture is dominated by a ductile mechanism on the other hand Figs.(10) (a) and(b) show the tensile fracture obtained on specimens of the Aluminum alloy 7020 solution treated at 450 °C for 2.5 hrs followed by a single aging cycle at 150 °C for 5 hrs. the analysis of these fractures indicate the coexistence of a substantial cleavage mode together with the existing dominating dimple modes. This indicates that the ductility of such specimens is relatively lower while its strength is higher which is inconformity with the obtained mechanical results more over Fig (11) (a) & (b) demonstrates the tensile fracture obtained on specimens of the aluminum alloy 7020 solution treated at 450 °C for 2.5 hrs. followed by a low temperature aging cycle at 120 °C for 6 hrs then another high temperature aging cycle at 150 °C for 7 hrs. we can note the existence of dominating dimple ductile fracture, limited areas of cleavage fracture, and some zones where intergranular fracture and precipitates breakage can be visualized.

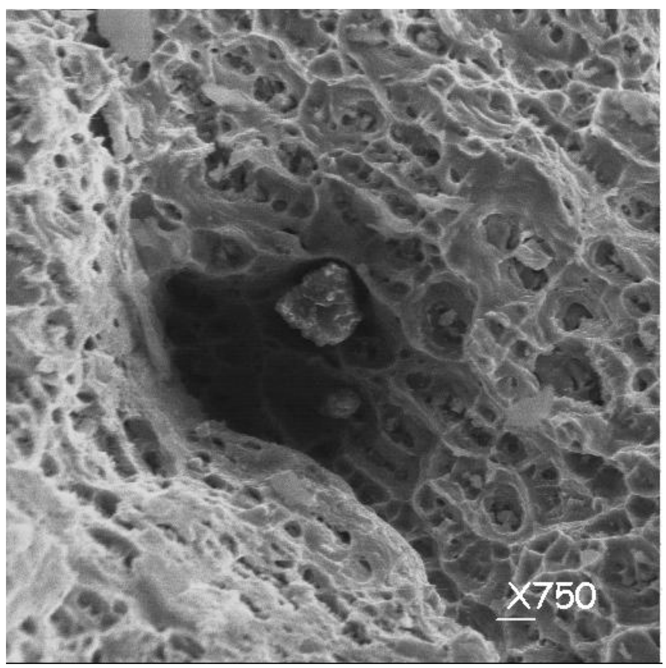

(a)

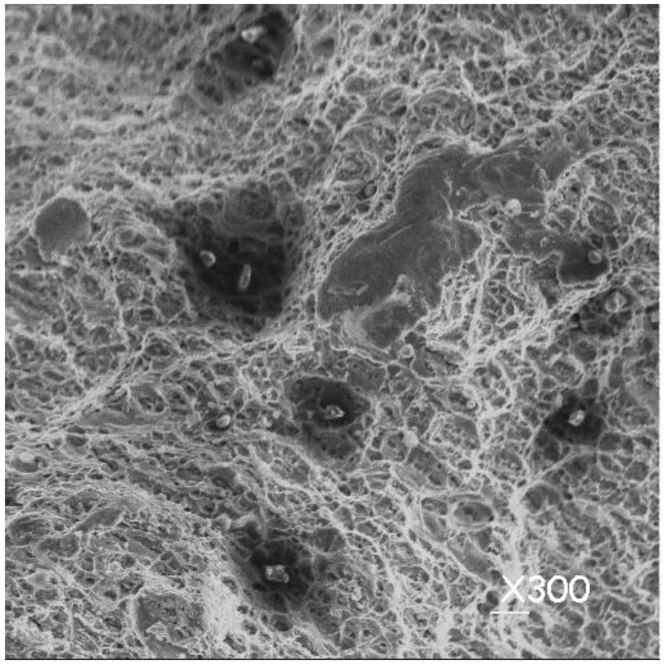

(b)

Fig. 9 Fracture surface of solution treated Al-Zn-Mg alloy type 7020

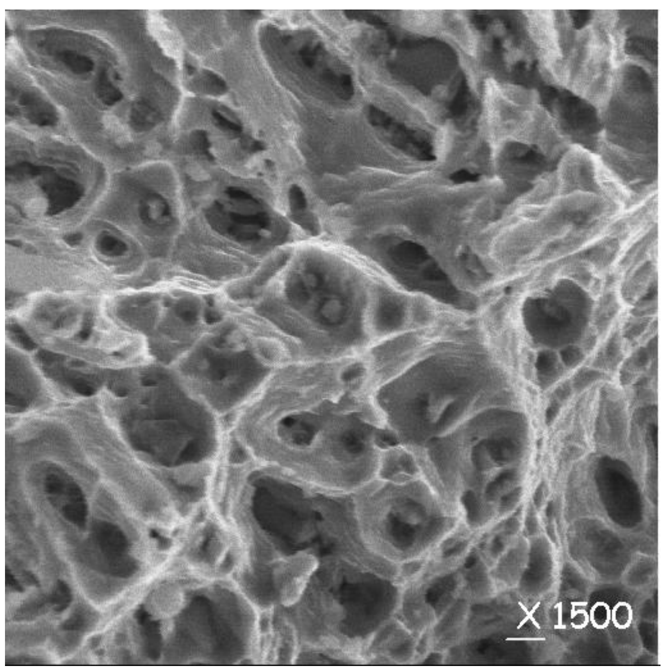

(a)

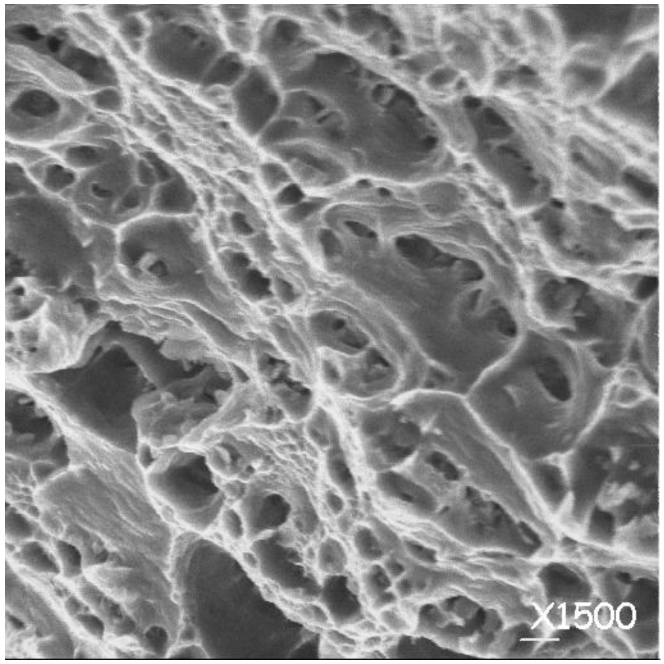

(b)

Fig. 10 Fracture surface of solution treated Al-Zn-Mg alloy type 7020

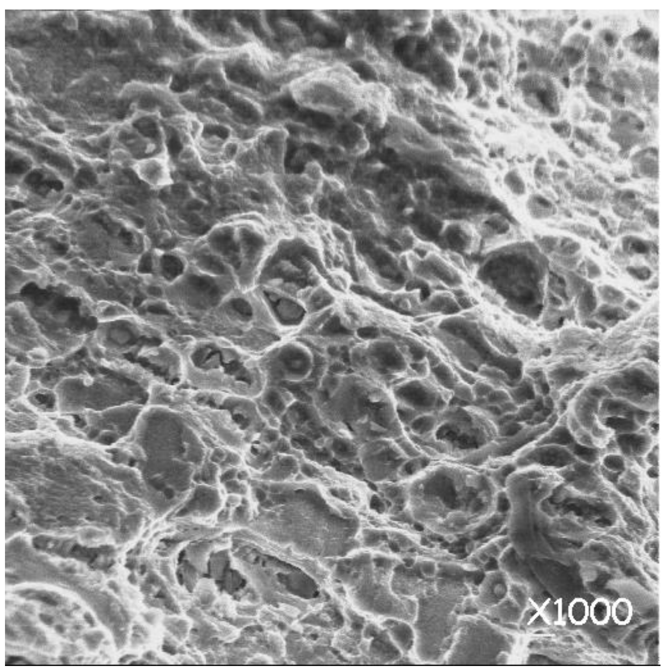

(a)

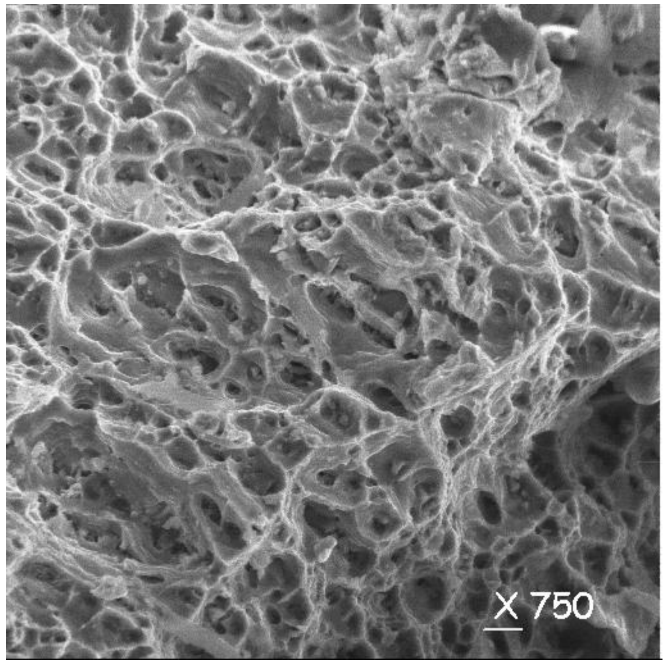

(b)

Fig. 11 Fracture surface of solution treated Al-Zn-Mg alloy type 7020

4. Conclusion

(1) Natural aging treatment results in a hardness peak of 113 HB after 50 days while the solution treated specimen results a hardness value of 54 HB; there is a significant increase in hardness properties during the first five days of natural aging due to nucleation of GP zones, then the rate of strengthening decrease.

(2) The hardness gain when the aging time in prolonged to 70 days can be neglected then natural aging beyond 50 days is not worthy
(3) As the aging temperatures increases the aging time to reach the peak hardness decreases, moreover the value of at this peak hardness decreases. On the other hand, it can be noted that artificial aging above 150 °C results in relatively low peak hardness values which can be manifested at very low aging times less than 45 min.

(3) One-step aging of the alloy results in a peak UTS value of 350 and 320MPa, while the resulted hardness peak values were 109, 95 after 28 hrs aging at 120°c and 5 hrs aging at 150°c respectively.

(4) Serrated behavior is manifested in the case of solution treated state and is recognized that it is a locking type A serration mechanisms, while in specimens aged at 120 °C and 150 °C, we cannot reveal any visible serrated behavior.

(5) The tow-stags aging can provide the advantages of both low and high aging temperatures. Where the low temperature allow the formation of a large number of nucleation sites, while high aging temperature increase the rate of growth to reduce the aging time.

(6) The peak values of the aging curves in tow-step aging depend greatly on the aging time of low temperature aging cycle. Nucleation and growth to GP zones takes about 6 hrs aging at 120 °Cand the further aging time at this low aging temperature spend in growth of this nuclei to form η' then η.

5. References

[1] Ian J. Polmear, *Light alloys from traditional alloys to nanocrystals*, 4th. ed., Vol. 1, Elsevier, Australia, 2006

[2] Material Characterization 46 (2001) 251-257 “Structural parameters of 7020 alloy after heat treatment simulating the welding process”, 28 December 2000, Poland, 13 February 2001.

[3] Hawrylkiewicz S., Lech-Grega M., Richert M, Szymański W., “Quantitative change in structure parameters of 7020 alloy after heat treatment simulating the welding process,” ”, *Proceedings of the 6th International Conference on Stereology and Image Analysis in Materials Science”* September, 2000, pp. 167-72.

[4] Aca Material 51 (2003) 5151-5158 “Secondary precipitation in Al-Zn-Mg-(Ag) alloys”, 28 March 2003, Australia, 27 June 2003.

[5] Aca Material 51 (2003) 6077-6094 “Characterization and modeling of precipitate evolution in an Al-Zn-Mg alloy during non-isothermal heat treatments”, 2 June 2003, France, 23 July 2003.

[6] Materials science & Engineering A334 (2002) 1-5 “Pre-precipitation study in the 7012 Al-Zn-Mg-Cu alloy by electrical resistivity”, 9 August 2000, Brazil, 15 May 2001.

[7] M. Maher Osman, MSc thesis “Effect of thermal and thermo-mechanical treatments on the mechanical and fracture characteristics of Al-Cu and Al-Mg-Si alloys”, MTC, Cairo, Egypt, 1997.

[8] Vadim S. Zolotorevsky, *Casting Aluminum Alloys*, 1st. ed., Elsevier, Moscow, 2007.

[9] Askland.

[10] Aca Material 49 (2001) 3443-3451 “GP-zones in Al-Zn-Mg alloys and their role in artificial aging”, 14 February 2001, Sweden, 15 June 2001.

[11] Aca Material 52 (2004) 4503-4516 “Early-stage precipitation in Al-Zn-Mg-Cu alloy (7020)”, 27 February 2004, England, 6 June 2004.

[12] A. M. El Sheikh, “Precipitation Hardening and Substructures feature in Al-Zn-Mg alloys,” ”, *Proceedings of the strength of metals and alloys, ICSMA-7,”* 1985, pp. 483-488.

[13] M. Hörnqvist and B. Karlsson “Dynamic strain aging effects in an extruded AA7030 alloy subjected to tensile deformation”, Göteborg , Sweden, 1996.

[14] Journal De Physique IV October (1991) “Strain rate dependence on mechanical properties in some commercial aluminum alloys”, Japan.

[15] Metallurgical and Materials Transactions B 4 (1973) 523-517 “Serrated flow in Aluminum 6061 alloy”, 15 May 1972, USA.

[16] Aca Material 50 (2002) 2319-2329 “Precipitation sequence during quenching of the AA7010 alloy”, 14 April 2001, France, 14 January 2002.